

---

**MAGNETISM  
AND FERROELECTRICITY**

---

# Temperature Dependence of the Fine Structure of the *C* and *E* Absorption Bands in $\text{RbMnF}_3$ below the Néel Temperature

A. V. Malakhovskii and T. P. Morozova

*Kirensky Institute of Physics, Siberian Division, Russian Academy of Sciences,  
Akademgorodok, Krasnoyarsk, 660036 Russia*

*e-mail: malakha@iph.krasn.ru*

Received February 3, 2005; in final form, April 28, 2005

**Abstract**—The variation in the parameters (width, position, intensity) of the fine structure lines in the  $C[{}^6A_{1g} \rightarrow {}^4A_{1g}, {}^4E_g({}^4G)]$  and  $E[{}^6A_{1g} \rightarrow {}^4E_g({}^4D)]$  bands in  $\text{RbMnF}_3$  with temperature is studied in the temperature range 10–70 K. In the *C* band, two narrow ( $<6 \text{ cm}^{-1}$ ) lines are distinguished at distances of 77 and  $80 \text{ cm}^{-1}$  from the exciton line at  $T = 10 \text{ K}$ . The other lines in the *C* band and all lines in the *E* band are more than  $20 \text{ cm}^{-1}$  wide. It is demonstrated that the narrow lines become allowed because of the spin-exchange interaction within a long-range magnetic order model and originate from the excitation of exciton–magnon bound states and that the other lines are made allowed by the exchange–vibronic mechanism within a short-range magnetic order model and originate from the excitation of bound states composed of an exciton, magnon, and odd-parity phonon. The vibrational replicas of the main exciton–magnon–phonon lines are due to the quadratic vibronic interaction with odd-parity vibrations. Variations of the intensities and widths of the absorption lines with temperature indicate that these parameters are affected by relaxation and delocalization of the bound states.

PACS numbers: 78.20.–e, 78.40.Ha, 75.50.Ee

DOI: 10.1134/S1063783406020156

## 1. INTRODUCTION

The behavior of spin-forbidden *d–d* transitions, which include all *d–d* transitions in the  $\text{Mn}^{2+}$  ion, is directly related to the mechanisms that make them allowed by spin and parity. Spectra of the  $C[{}^6A_{1g} \rightarrow {}^4A_{1g}, {}^4E_g({}^4G)]$ , and  $E[{}^6A_{1g} \rightarrow {}^4E_g({}^4D)]$  bands in  $\text{RbMnF}_3$  have been much studied. In particular, measurements in a magnetic field have revealed [1] that all lines in the *C* band are cooperative in character (photons are absorbed by exchange-coupled ions belonging to two sublattices). However, the role of vibrations in the formation of the spectrum of magnetically ordering compounds is unclear. Odd vibrations ( $4t_{1u} + t_{2u}$  in  $\text{RbMnF}_3$  [2]) provide an efficient mechanism for making transitions parity-allowed and cannot be ignored. Accordingly, in magnetically ordering compounds, there are two ways to make spin-forbidden *d–d* transitions allowed: the exchange interaction [3] and exchange-vibronic mechanism (see [4, 5, p. 108]). In particular, both should be taken into account when the nature of the lines in the *C* and *E* bands of  $\text{RbMnF}_3$  is discussed. The absorption of light in crystals is usually described in terms of quasiparticles. We discuss the peculiarities of this representation in relation to our experimental results for the case where several excita-

tions (electronic, magnetic, and vibrational) are simultaneously required to make the optical absorption for spin-forbidden *d–d* transitions allowed.

## 2. EXPERIMENT

The crystal lattice of  $\text{RbMnF}_3$  has a perovskite structure belonging to the cubic symmetry group  $O_h^1$ . The crystal becomes antiferromagnetic at  $T_N = 82.5 \text{ K}$ . Our sample was cut in the (100) plane and was 1-mm thick. Measurements were performed in a flow-through quartz cryostat fitted with flat fused-quartz windows. Cooling was provided by a flow of helium vapor from a Dewar flask. The temperature was controlled to within  $\pm 0.2 \text{ K}$ . The sample was placed directly in the gas flow.

The absorption spectra (shown in Figs. 1, 2) were obtained in nonpolarized light using the two-beam modulation technique [6]. Two light beams, one of which went through and the other by the sample, were alternately passed through a photomultiplier by a vibrational light chopper. The signal from the photomultiplier was passed through a logarithmic amplifier. As a result, the alternating part of the signal at the amplifier output was proportional to the optical density of the

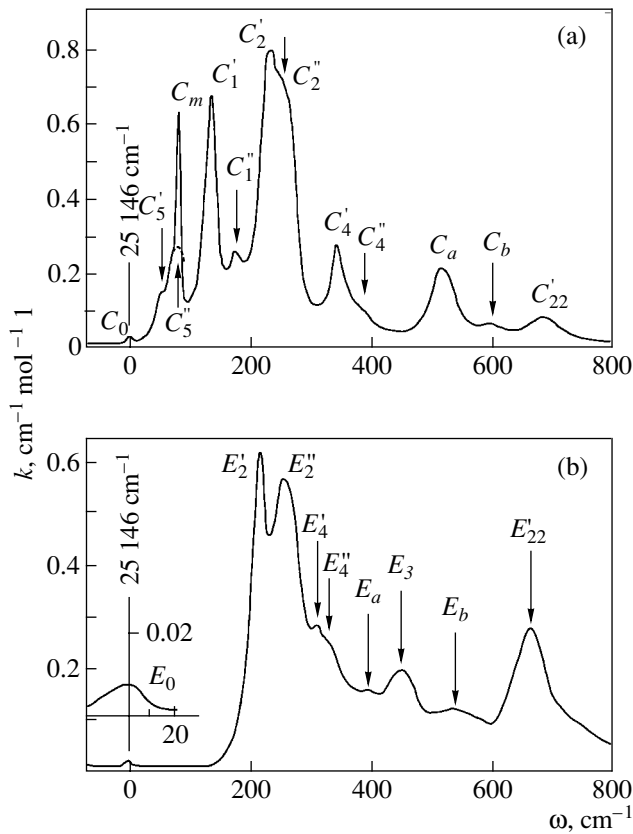


**Fig. 1.** Spectra of the (a)  $C$  and (b)  $E$  absorption bands in  $\text{RbMnF}_3$  at  $T = 10$  K. The  $C_5''$  line is shown by a dashed line in frame (a). Energies are measured from the exciton line energies indicated. The inset to panel (b) presents the exciton line in an expanded scale.

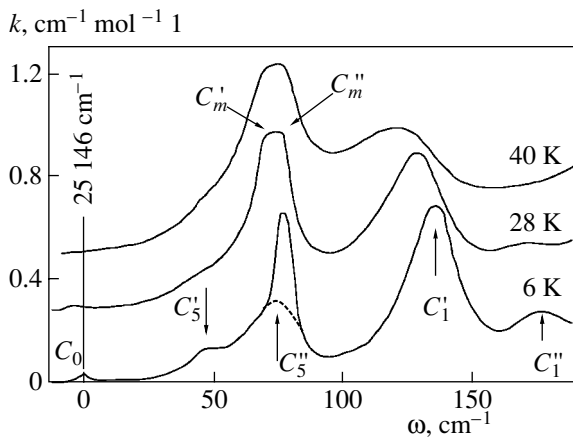


**Fig. 2.** Variation of part of the  $C$  band spectrum with temperature. The  $C_5''$  line is shown by a dashed line. The energy is measured from the exciton line energy indicated.

sample. This technique has great advantages for studying weak absorption lines. Thanks to it, we managed to reliably detect a very weak exciton line  $E_0$  (Fig. 1b). We

recorded spectra using an optical gap of  $\sim 4$   $\text{cm}^{-1}$  around the  $C$  band and  $\sim 8$   $\text{cm}^{-1}$  around the  $E$  band. Data were recorded using a computerized setup based on a DFS-8 spectrograph.

The absorption spectra were decomposed into elementary components by the method of least squares using a computer. The positions, widths, amplitudes, and shapes of the components could be varied. The lineshape could be changed (from a Gaussian to a Lorentzian profile) independently to the left and to the right of the peak frequency. The variable shape of the absorption lines was described by a Taylor series with a finite number of terms [7]. In particular, it is found that, at low temperatures, the left side of the  $C_1'$  line (Figs. 1a, 2) is described well by a Lorentzian, its right side is close to a Gaussian, and the  $C_4'$  line has a symmetric Lorentzian shape.

### 3. EXPERIMENTAL RESULTS AND INTERPRETATION OF THE ABSORPTION SPECTRA

All lines in the  $C$  band spectra (Fig. 1a), apart from the exciton line  $C_0$ , are due to cooperative (two-sublattice) absorption, which is convincingly demonstrated by the fact that these lines do not split in a magnetic field [1]. We are not aware of any analogous experiments concerning the  $E$  band; however, it is quite reasonable to assume that the  $E$  band is likewise due to cooperative absorption, because its intensity is almost identical to that of the  $C$  band (Figs. 1, 2) and the intensity of the spin-forbidden  $d-d$  absorption bands that are made allowed by exchange interaction are strongly enhanced.

As we noted above, there are two exchange-related mechanisms through which spin-forbidden  $d-d$  transitions become allowed: the exchange and exchange-vibronic mechanisms. In magnetically ordering compounds, the first mechanism gives rise to exciton-magnon lines and the second, to exciton-magnon-phonon lines (involving odd-parity phonons). The spin selection rule is broken in both cases identically, namely, due to the exchange interaction, whereas the parity selection rule can be broken in different ways in centrosymmetric crystals. In the case of the exchange-vibronic mechanism, this selection rule is broken due to the vibronic interaction with odd-parity vibrations, and, in the case of the exchange mechanism, the selection rule is broken without the assistance of vibrations but rather because a pair that absorbs a photon has no inversion center in the excited state. The second mechanism is obviously much less efficient; therefore, the exciton-magnon lines have to be much weaker than the exciton-magnon-phonon lines.

There are two models describing the exchange mechanism through which electron transitions become spin-allowed: a long-range order model (Fig. 3a) and a

short-range order model (Fig. 3b), which are named by analogy with similar models describing magnetic ordering. In the first model, the ion states are split in the effective exchange field according to the spin projection  $M_S$  onto the ordering direction. The electron transition becomes allowed with respect to the spin projection of an ion pair because the spin projection of an ion located near the optically excited ion changes. According to this model, if the exchange interaction is antiferromagnetic, then the energy of the “cold” exciton–magnon electric-dipole transition (which does not change the spin projection of the pair) should exceed the energy of the excitonic magnetic-dipole transition (which changes the spin projection of the pair) by the energy of a magnon at the edge of the Brillouin zone. Furthermore, this energy difference should vary with temperature in proportion to the magnetic moment of the sublattice.

In the short-range order model, the exchange interaction of an ion pair is taken into account exactly and the effect of the rest of the crystal is included by introducing an effective field, which not only splits the states of the pair according to the projection of its total spin but also mixes the states that have different total spins  $S$  ( $\Delta S = 1$ ) but identical projections  $M_S$  [8]. According to this model, the magnetic-dipole (with a change in  $S$ ) and electric-dipole (without a change in  $S$ ) transitions have the same energy at  $T = 0$  K. Indeed, at  $T = 0$  K, the lowest and the only populated state is a superposition of the states with identical values  $M_S = 0$  but with different total spins,  $S = 0$  and 1. Therefore, both kinds of transitions can occur from the lowest level.

In the long-range order model, as the temperature increases from 0 K to  $T_N$ , the intensity of the cold exciton–magnon absorption that is allowed by spin because of the exchange interaction strongly decreases [9], whereas in the short-range order model its intensity increases. Therefore, the predictions from these two models are substantially different and experiment will help distinguish between them.

The probability of exchange–vibronic absorption can be written as (see [4, 5, p. 109])

$$W_{ev} = kW_eW_v, \tag{1}$$

where  $W_e$  and  $W_v$  are the probabilities of the exchange and vibronic absorptions, respectively (the first value disregards the parity selection rule, and the second, the spin selection rule), and  $k$  characterizes the coupling between the two processes. As is well known, the temperature dependence of the vibronic absorption is given by

$$W_v \sim \coth(\Omega/kT), \tag{2}$$

where  $\Omega$  is the frequency of the odd-parity vibration that makes the transition allowed. For the odd vibrations in  $\text{RbMnF}_3$  [11, 12] (see table), the function given by Eq. (2) is almost constant in the temperature range under study. Therefore, in a first approximation, the

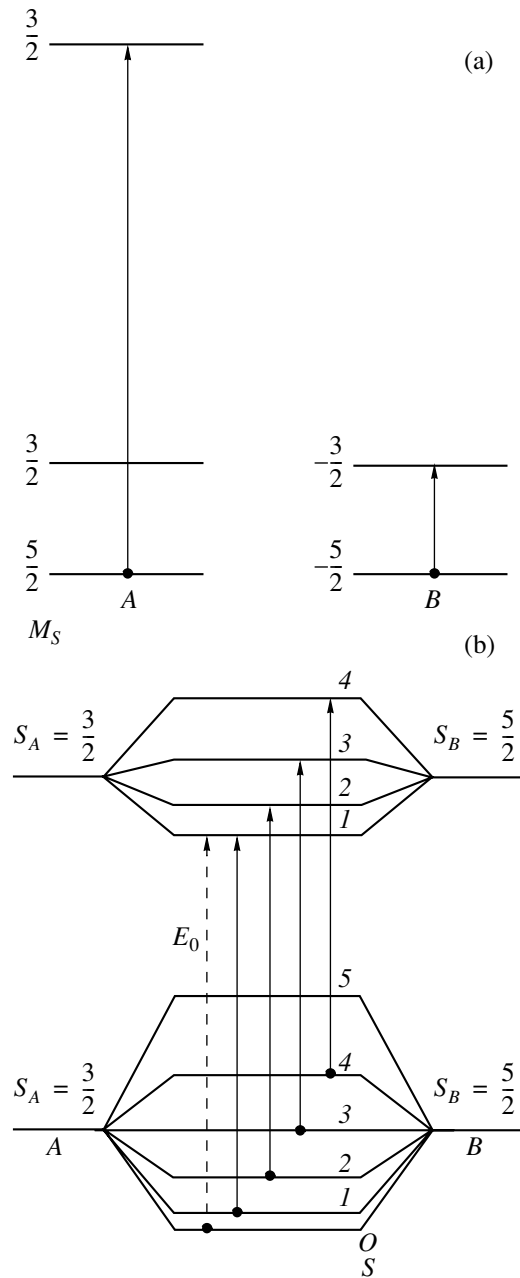


Fig. 3. (a) The long-range and (b) short-range order models.

temperature dependences of the intensities of the observed absorption lines should be determined by the exchange mechanism. However, the temperature dependence of the intensities of the exchange (and exchange–vibronic) absorption is determined not only by variations in the populations of levels and in the mixing of states as described above (see below).

If a photon is absorbed by an atom of a periodic lattice, the electronic, vibrational, or spin excitation will travel through the crystal as a quasiparticle: an exciton, phonon, or magnon. Depending on the coupling between them, the quasiparticles can exist either in a

Energies ( $\Omega_1$  to  $\Omega_5$ ) of vibration quanta in  $\text{RbMnF}_3$  (measured in  $\text{cm}^{-1}$ ) as determined from IR spectra recorded at  $T = 85$  K [11, 12] and from optical absorption spectra (Figs. 1, 2)

Energy	Vibration	Transverse		Longitudinal		C band		E band	
		$k \approx 0$	$k_{\max}$	$k \approx 0$	$k_{\max}$	$C'$	$C''$	$E'$	$E''$
$\Omega_1$	$t_{1u}$	111	109	126	120	137	179	–	–
$\Omega_2$	$t_{1u}$	194	193	267	224	232	264	218	261
$\Omega_3$	$t_{1u}$	396	386	469	434	–	–	461	461
$\Omega_4$	$t_{2u}$		311			346	390	313	320
$\Omega_5$	$t_{1u}$	0	80	0	90	72	48	–	–

free or a bound state. If quasiparticles are free, highly mobile, and strongly delocalized, their interaction per photon-absorbing cluster is almost zero and the probability of many-particle absorption is likewise very low. (By definition, completely free quasiparticles do not interact.) However, the exciton, magnon, and phonon can form a bound, localized, slow-moving excitation, which does not differ greatly from the corresponding impurity excitation [13–15]. The probability of the optical transition into the stable bound state is proportional to the probability that the superposed configuration (in which all excitations in question are on the same site) exists as a component in the delocalized bound state. The probability of the transition into the superposed configuration is described by the local (cluster) models of the mechanisms (described above) through which electronic transitions become allowed.

So, if exciton–magnon or exciton–magnon–phonon absorption is observed in a periodic crystal, this means that a fairly stable bound exciton–magnon or exciton–magnon–phonon (or biexciton [15]) state is created when a photon is absorbed. The properties of this absorption, in a first approximation, can be described by the local (cluster) models. However, even a stable bound state inevitably relaxes and disintegrates into free quasiparticles. The relaxation rate in this case, in a first approximation, is the sum of the relaxation rates of all excitations involved in the bound state. Therefore, the width of the exciton–magnon line should be significantly smaller than the width of the exciton–magnon–phonon line. The widths of the absorption lines can also increase due to the delocalization of the bound states. The delocalization transforms a monochromatic, purely local excitation into an energy band of quasi-local excitations. This line broadening is independent of temperature in a first approximation, whereas the broadening due to relaxation is strongly dependent on temperature. A combination of these factors can explain the variety of temperature dependences of the linewidths (Fig. 4).

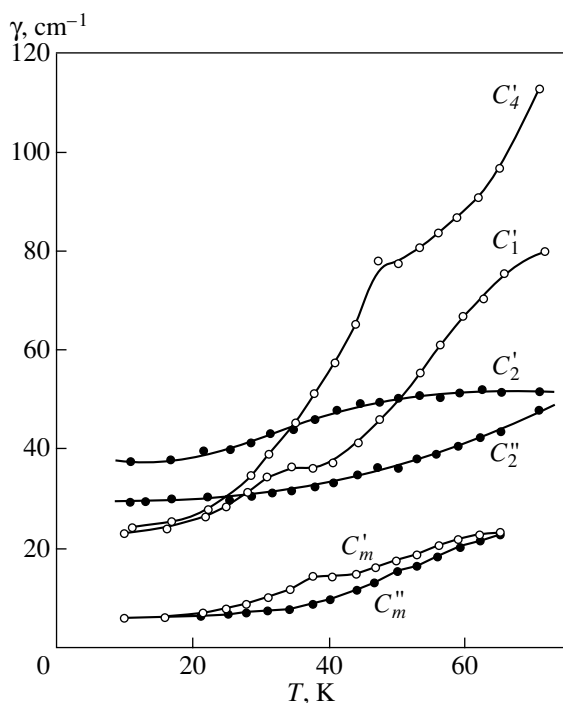
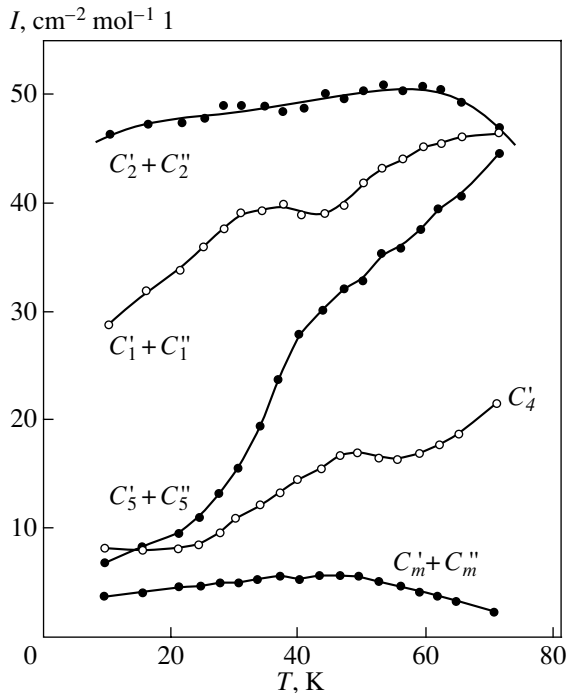
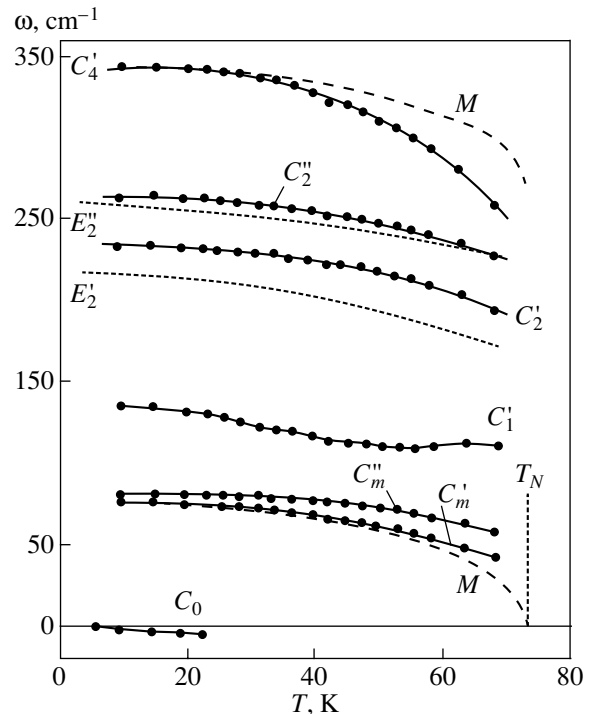


Fig. 4. Widths of lines in the C band as a function of temperature.

Up to now, the band near  $80 \text{ cm}^{-1}$  in the C spectrum (Figs. 1a, 2) was assumed to be a single line. As is shown in Fig. 2, here there are four lines that differ quite markedly in terms of their properties. Two of them,  $C'_m$  and  $C''_m$ , are the narrowest (Figs. 1a, 4) and least intense (Fig. 5) in the C band. At  $T = 10$  K, these lines have energies of  $77$  and  $80 \text{ cm}^{-1}$  (the exciton line  $C_0$  is taken as the origin), which are close to the energy of a magnon at the edge of the Brillouin zone ( $72 \text{ cm}^{-1}$ ), and their intensities decrease significantly as  $T \rightarrow T_N$  (Fig. 5). These features, according to the above discussion, are sufficient to attribute the  $C'_m$  and  $C''_m$  lines to exciton–magnon lines described by the long-range order model. However, it is seen in Fig. 6 that the temperature dependences of the frequencies of the  $C'_m$  and  $C''_m$  lines do not differ substantially from those of the other lines and do not follow the temperature dependence of the magnetic moment  $M$ , as they seemingly should according to the long-range order model. Such a discrepancy has already been observed. For example, in



**Fig. 5.** Intensities of lines in the  $C$  band as a function of temperature.



**Fig. 6.** Variation of the frequencies of spectral lines with temperature.

the trigonal antiferromagnet  $\text{FeCO}_3$  with large uniaxial anisotropy, where the exciton line is observed over a wide temperature range, the distance between the excitonic and exciton-magnon lines is independent of temperature even at  $T > T_N$  [16]. A feature is observed in the temperature dependence of the  $C_m'$  linewidth near 40 K (Fig. 4). Approximately at the same temperature, the position of the luminescence maximum experiences a jump, which has been attributed to magnetic ordering of the  $\text{Mn}^{2+}$  ion in the excited state and the surrounding ions in the ground states [17]. There is no exciton-magnon line in the  $E$  band. All other lines in the  $C$  and  $E$  bands are much wider (Fig. 1) and, for the most part, their intensities are higher (Figs. 5, 7) than those of the  $C_m'$  and  $C_m''$  lines and, as a rule, increase with temperature. Therefore, all the wide lines can be assumed to be exciton-magnon-phonon lines and to be made spin-allowed according to the short-range order model.

The frequencies of different lines vary with temperature in different ways. For example, as the temperature increases from 10 to 70 K, the frequencies decrease by values ranging from  $17 \text{ cm}^{-1}$  for  $C_m''$  to  $80 \text{ cm}^{-1}$  for  $C_4'$  (Fig. 6). This observation suggests that the shift of the lines is probably due to the variation not only in the effective exchange field but also in the frequencies of quasi-local vibrations.

In the case of exciton-magnon-phonon absorption, the  $d-d$  transitions are made parity-allowed because of

the mixing of odd and even electronic states caused by vibronic interaction with odd-parity vibrations (the matrix elements of the part of the vibronic Hamiltonian linear in the vibrational coordinate  $q$ ,  $V \sim q$ , taken between various electronic terms are nonzero). The diagonal matrix elements of the linear part of the vibronic Hamiltonian are exactly zero for odd vibrations. Consequently, the adiabatic potential does not shift for these coordinates during the electron transition and only one quantum of an odd vibration can (and must) be excited in the electron transition that is made parity-allowed.

The diagonal matrix elements of the quadratic part of the vibronic Hamiltonian  $V \sim q^2$  are nonzero both for even and odd vibrations and can change during an electron transition (i.e., the frequency of the vibration changes). In this case, any odd number of odd-parity vibration quanta can be excited during the  $d-d$  transition (let us recall that only odd vibrations exist in  $\text{RbMnF}_3$ ). If the matrix elements of the part of the vibronic Hamiltonian  $V \sim q_1 q_2$  (where  $q_1$  and  $q_2$  are different symmetrized coordinates) are nonzero and change during the electronic transition, then the normal coordinates are mixed (the Dushinskii effect [18]) and lines can arise at heterodyne vibration frequencies (with the participation of quanta of different vibrations) [19–21].

If a vibronic interaction diagonal with respect to electronic terms involves a degenerate electronic state, then the adiabatic potential of this level splits. The

number of sheets of the split adiabatic-potential surface is equal to the degeneracy of the electronic level [22]. If (as in our case) there is only quadratic vibronic interaction, these sheets differ only in terms of their curvature. In this case, the vibrational and the corresponding electron–vibration states split according to the degeneracy of the electronic level (that is, they split into two states in the case of the  $A_{1g} \rightarrow E_g$  transition).

The matrix element of an electric-dipole transition that is made allowed by an odd vibration can be written as

$$D_{if} \sim \varphi_i^*(D\Delta V_q)\varphi_f dr, \quad (3)$$

where  $\Delta V_q$  is the linear part of the vibronic Hamiltonian corresponding to the vibrational coordinate  $q$  and  $\varphi_i$  and  $\varphi_f$  are the initial and final electronic states, respectively.

In order for the integral in Eq. (3) to be nonzero, the representation of the integrand has to contain a fully symmetric representation:

$$A_{1g} \in \Gamma_i \times \Gamma_D \times \Gamma_q \times \Gamma_f. \quad (4)$$

Using Eq. (4) and the representation multiplication table, it is easy to find that, from the symmetry point of view, in the  $O_h$  group, the vibrations  $t_{1u}$  and  $t_{2u}$  are equally effective in making all transitions (except  $A_{1g}, A_{2g} \rightarrow A_{1g}, A_{2g}$ ) allowed. For the  $A_{1g} \rightarrow A_{1g}$  and  $A_{2g} \rightarrow A_{2g}$  transitions, the vibration  $t_{1u}$  is active, and, for the  $A_{1g} \rightarrow A_{2g}$  transition, the vibration  $t_{2u}$  is active. Using Eq. (3) we can also establish [5, p. 75] the orientation of the active components of vibrations with respect to the vector  $\mathbf{E}$  of a light wave. For example, in the  $O_h$  group, for the  $A_{1g}, A_{2g}, E_g \rightarrow A_{1g}, A_{2g}, E_g$  transitions, the components  $q \parallel \mathbf{E}$  of the  $t_{1u}$  and  $t_{2u}$  vibrations are active, and the components  $q \perp \mathbf{E}$  are active for the  $A_{1g}, A_{2g}, E_g \rightarrow T_{1g}, T_{2g}$  transitions; that is, vibrations along the direction of propagation of light are also active. All components of the vibrations mentioned above are active for the  $T_{1g}, T_{2g} \rightarrow T_{1g}, T_{2g}$  transitions. Thus, for the  $A_{1g} \rightarrow A_{1g}, E_g$  transitions in which we are interested, only the transverse vibrations are active and the observed splitting of the exciton–magnon–phonon transitions (lines denoted by primes and double primes in Figs. 1 and 2) must be related to the splitting of the vibronic functions in the excited state caused by the quadratic diagonal vibronic interaction with the  $E_g$  state. Moreover, in contrast to direct absorption of IR photons by collective lattice modes, where propagating vibrations should be divided into longitudinal and transverse vibrations, in our case this classification carries no meaning. Indeed, as mentioned above, an absorbed optical photon creates a local bound state of electronic, vibrational, and magnetic excitations and only the relative orientation of the vibrations and the electric field vector of the light wave is important in this process.

In the short-range order model, as shown above, the magnetic-dipole purely excitonic transition (with a change in spin) and electric-dipole transition (without a change in spin) have the same energy at  $T = 0$  K if the vibrational mechanism for making them parity-allowed is not taken into account. Therefore, the energies of exciton–magnon–phonon lines reckoned from  $C_0$  (or  $E_0$ ) have to be equal to the energies of the local vibrational excitations involved in the bound states. We can take the frequencies of free lattice phonons in  $\text{RbMnF}_3$  obtained from IR absorption spectra (see table) as initial data for the purpose of line identification. These values, of course, can only be used tentatively, since the vibrations under discussion belong to the excited electronic states of an atom and are coupled to this dynamic defect in space; in other words, these vibrations are local or, more precisely, quasi-local. The identification thus obtained is presented in the table, where the lines are numbered in accordance with the numbers of active vibrations.

In the case of the  $C$  transition, because of the fact that, in a crystal field of  $O_h$  symmetry, there are two states with the same energy,  ${}^4E_g$  and  ${}^4A_{1g}$ , the quadratic vibronic interaction introduces additional changes into the frequencies of quasi-local vibrations at the electronic transition. Vibrations with frequencies lying in the acoustic-vibration range also appear in the  $C$  band spectrum ( $C'_5$  and  $C''_5$  in Fig. 2). Of course, these are not collective lattice modes but rather quasi-local vibrations near the cluster that absorbs light and their spectrum is different from the true acoustic vibrations of the crystal.

Changes in vibration frequencies during an electronic transition are evidence that the vibration wave functions are also modified, which gives rise to the appearance of additional lines due to the excitation of an odd number ( $n > 1$ ) of odd-parity vibrations quanta. We have  $C'_{22} = 3\Omega'_2$  and  $E'_{22} = 3\Omega'_2$  to within experimental accuracy, where  $\Omega'_2$  is found using the  $C'_2$  and  $E'_2$  lines, respectively (see table).

Replicas of the exciton–magnon lines separated by a distance of 470–480  $\text{cm}^{-1}$  (equal to  $2\Omega'_2$ ) are observed in  $\text{RbMnF}_3$  in the  ${}^6A_{1g} \rightarrow {}^4T_{1g}$  and  ${}^4T_{2g}$  absorption bands [23]. The  $C_a, C_b, E_a,$  and  $E_b$  lines are not as well identified. If we assume that  $C_a = 3\Omega'_1$  and  $C_b = 3\Omega''_1$ , we get  $\Omega'_1 = 173 \text{ cm}^{-1}$  and  $\Omega''_1 = 200 \text{ cm}^{-1}$ , which are significantly differ from the values obtained using the main lines (see table). Better quantitative agreement is obtained using the identification  $C_a = C'_2 + 2\Omega'_1$  and  $C_b = C'_2 + 2\Omega''_1$ , where  $\Omega'_1 = 144 \text{ cm}^{-1}$  and  $\Omega''_1 = 168 \text{ cm}^{-1}$  (cf. table). This identification implies the existence of replicas of lines at heterodyne frequencies, which suggests the Dushinskii effect. If we

assume that  $E_a = 3\Omega_1'$  and  $E_b = 3\Omega_1''$ , then  $\Omega_1' = 132 \text{ cm}^{-1}$  and  $\Omega_1'' = 180 \text{ cm}^{-1}$ , which is in good agreement with the frequencies obtained using the  $C$  band. However, the  $E$  spectrum has no main lines at these frequencies; so the appearance of higher harmonics is doubtful. Considering these lines, similar to  $C_a$  and  $C_b$ , to be the combinations  $E_a = E_2' + 2\Omega_1'$  and  $E_b = E_2'' + 2\Omega_1''$ , we obtain  $\Omega_1' = 90 \text{ cm}^{-1}$  and  $\Omega_1'' = 140 \text{ cm}^{-1}$ .

Let us return to the temperature dependence of the intensities. If this dependence were determined only by the population and mixing of the exchange-split terms, as described above, then the intensities of all exciton-magnon-phonon lines would vary with temperature in the same manner (in the temperature range under study). However, this is not the case (Figs. 5, 7). It is shown in [15, p. 123] that the intensity of this kind of absorption and its variation with temperature depend on the relaxation rate of bound excitations. In particular, considering only the direct relaxation to the phonon reservoir, we can describe the probability of the exchange-vibronic absorption by the formula

$$W_{\text{ev}} = W_0 \{ V(J) [1 - \exp(-J/kT)]^{-1} + V(\Omega) [1 - \exp(-\Omega/kT)]^{-1} \}^{-1} \coth(\Omega/2kT). \quad (5)$$

Here,  $W_0$  is the probability of the exchange-vibronic transition into a completely stable bound exciton-magnon-phonon state calculated accounting for the population and mixing of the exchange-split levels;  $J$  and  $\Omega$  are the energies of the magnetic and vibration excitations, respectively;  $V(J) \sim B_J f(J)$  and  $V(\Omega) \sim B_\Omega \Omega f(\Omega)$  are parameters characterizing the interaction of the respective excitations with lattice phonons;  $B_J$  and  $B_\Omega$  are the Einstein coefficients for the stimulated emission of phonons; and  $f(J)$  and  $f(\Omega)$  are the phonon densities of state.

The probability of relaxation of an electronic excitation that corresponds to a forbidden transition is very small both for the cases of photon emission and decay into phonons; therefore, this probability is omitted in Eq. (5). Equation (5) is valid for a sufficiently large relaxation rate (see [5, p. 123]). For a small relaxation rate, we have

$$W_{\text{ev}} = W_0 \coth(\Omega/2kT). \quad (6)$$

It follows from Eq. (5) that, first, the absorption probability decreases as the coupling of magnetic and vibration excitations to lattice phonons is enhanced and, second, that the temperature dependence of this probability is related to the ratio of the relaxation rates of these excitations [the terms in square brackets in Eq. (5)]. The parameters  $V(J)$  and  $V(\Omega)$  depend not only on the Einstein coefficients but also on the phonon density of states at the frequencies of the respective excitations, which are modified in electronic transitions. That is why the temperature dependences of the intensities of

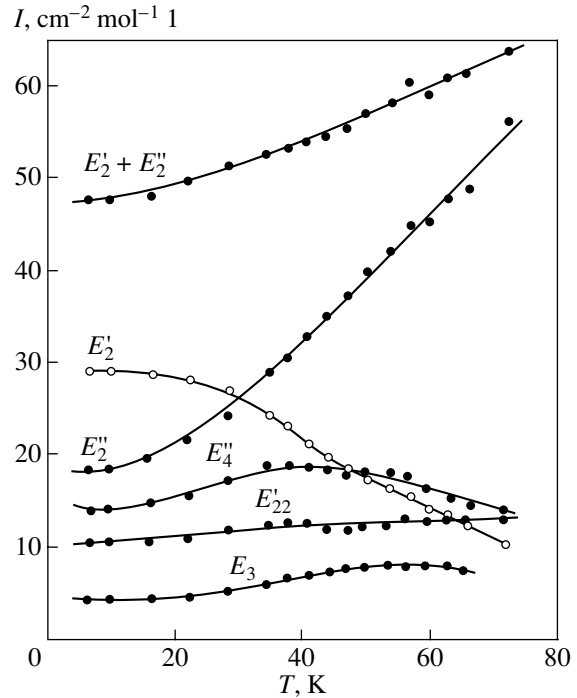


Fig. 7. Intensities of lines in the  $E$  band as a function of temperature.

spin-forbidden  $d-d$  transitions are so diverse both at  $T < T_N$  and at  $T > T_N$  and do not follow Eq. (6). The difference between the temperature dependences of the intensities of the  $E_2'$  and  $E_2''$  lines (Fig. 7) is an example of this situation. However, in impurity crystals, where magnetic excitations related to the exchange interaction are completely absent and the coupling of local impurity vibrations with lattice phonons is weak, the intensity follows Eq. (2).

We have to stress that some bound states (including the exciton-magnon state) that appear during the  $C$  transition do not appear during the  $E$  transition and vice versa (Fig. 1; see also table). The spectra of the  $C$  and  $E$  bands are qualitatively similar for  $\omega > 200 \text{ cm}^{-1}$ , and the lines observed in the  $C$  band at  $\omega < 200 \text{ cm}^{-1}$  do not appear in the  $E$  band. On these grounds, it may be assumed that the spectrum of the  $C$  band at  $\omega < 200 \text{ cm}^{-1}$  is due to the  ${}^6A_{1g} \rightarrow {}^4A_{1g}$  transition. However, the  ${}^6A_{1g} \rightarrow {}^4E_g({}^4G)$  exciton line  ${}^6A_{1g} \rightarrow {}^4A_{1g}$ , which was found in  $\text{K}_2\text{MnF}_4$  at a distance of  $350 \text{ cm}^{-1}$  from the  ${}^6A_{1g} \rightarrow {}^4E_g({}^4G)$  exciton, does not have a significant effect on the  $C$  band spectrum [24]. Therefore, almost the entire spectrum of the  $C$  band is related to the  ${}^6A_{1g} \rightarrow {}^4E_g$  transition and the difference between the  $C$  and  $E$  bands is due to the differences in the magnitude of the coupling between quasiparticles and in their relaxation rates for the respective transitions.

## 4. CONCLUSIONS

The variation in the parameters (width, position, intensity) of the fine structure lines in the  $C[{}^6A_{1g} \rightarrow {}^4A_{1g}, {}^4E_g({}^4G)]$  and  $E[{}^6A_{1g} \rightarrow {}^4E_g({}^4D)]$  bands in  $\text{RbMnF}_3$  with temperature has been studied in the temperature range 10–70 K. The exciton–magnon and exciton–magnon–phonon absorption lines have been identified. It has been demonstrated that the exciton–magnon lines are made allowed by the exchange interaction within the long-range magnetic order model and originate from the excitation of exciton–magnon bound states and that the exciton–magnon–phonon lines are made allowed by the exchange–vibronic mechanism within the short-range magnetic order model and originate from the excitation of bound states of an exciton, magnon, and odd phonon.

The vibrational replicas of the main exciton–magnon–phonon lines are due to the quadratic vibronic interaction with odd vibrations. The frequencies of the local vibrations in the excited electronic state differ from the frequencies of the collective lattice modes and are split because of the quadratic vibronic interaction with the doubly degenerate electron state  $E_g$ . The variations of the intensities and widths of the absorption lines with temperature indicate that they are affected by relaxation and delocalization of the bound states. Some of the bound states that are observed in the  $C$  band spectrum do not appear in the  $E$  band and vice versa. This fact can be explained by the difference between the relaxation rates and coupling constants of these states at the respective electronic transitions.

## REFERENCES

1. V. V. Eremenko, V. P. Novikov, and E. G. Petrov, *J. Low Temp. Phys.* **16** (5/6), 431 (1974).
2. G. R. Hunt, C. H. Perry, and J. Ferguson, *Phys. Rev. A: At., Mol., Opt. Phys.* **134** (3), 688 (1964).
3. Y. Tanabe, T. Moriya, and S. Sugano, *Phys. Rev. Lett.* **15** (6), 1023 (1965).
4. A. V. Malakhovskii, *Solid State Commun.* **60** (7), 591 (1986).
5. A. V. Malakhovskii, *Selected Problems in Optics and Magneto-Optics of Transition-Element Compounds* (Nauka, Novosibirsk, 1992) [in Russian].
6. A. V. Malakhovskii, V. S. Filimonov, and E. A. Goncharov, Preprint No. 434F, IF SO AN SSSR (Institute of Physics, Siberian Division, All-Union Academy of Sciences, Krasnoyarsk, 1987).
7. A. P. Kucherov, *Zh. Prikl. Spektrosk.* **41** (1), 79 (1984).
8. V. V. Druzhinin, R. V. Pisarev, and G. A. Karamysheva, *Fiz. Tverd. Tela (Leningrad)* **12** (8), 2239 (1970) [*Sov. Phys. Solid State* **12** (8), 1789 (1970)].
9. T. Fujiwara, W. Gebhardt, K. Petanides, and Y. Tanabe, *J. Phys. Soc. Jpn.* **33** (1), 39 (1972).
10. I. Harada and K. Motizuki, *Solid State Commun.* **11** (1), 171 (1972).
11. C. H. Perry and E. F. Young, *J. Appl. Phys.* **38** (12), 4616 (1967).
12. E. F. Young and C. H. Perry, *J. Appl. Phys.* **38** (12), 4624 (1967).
13. É. I. Rashba, *Zh. Éksp. Teor. Fiz.* **54** (2), 542 (1968) [*Sov. Phys. JETP* **27**, 292 (1968)].
14. M. A. Kozhushner, *Zh. Éksp. Teor. Fiz.* **60** (1), 220 (1971) [*Sov. Phys. JETP* **33**, 121 (1971)].
15. Yu. B. Gaididei and V. M. Loktev, *Phys. Status Solidi B* **62** (2), 709 (1974).
16. V. V. Eremenko, Yu. G. Litvinenko, A. A. Motornaya, V. I. Myatlik, and V. V. Shapiro, *Zh. Éksp. Teor. Fiz.* **65** (3), 1227 (1973) [*Sov. Phys. JETP* **38**, 608 (1973)].
17. E. W. Prohovsky, W. W. Holloway, Jr., and M. Kestigian, *J. Appl. Phys.* **36** (3), 1041 (1965).
18. F. Dushinskii, *Acta Physicochim. URSS* **7** (4), 551 (1937).
19. M. Wagner, *J. Chem. Phys.* **41** (12), 3939 (1964).
20. A. V. Lukashin, *Opt. Spektrosk.* **32** (4), 661 (1972).
21. B. D. Fainberg, *Opt. Spektrosk.* **52** (6), 1099 (1982) [*Opt. Spectrosc.* **52** (6), 663 (1982)].
22. I. B. Bersuker and V. Z. Polinger, *Vibronic Interaction in Molecules and Crystals* (Nauka, Moscow, 1983; Springer, Berlin, 1989).
23. E. I. Solomon and D. S. McClure, *Phys. Rev. B: Solid State* **9** (11), 4690 (1974).
24. R. W. Schwartz, J. A. Spencer, W. C. Yeakel, P. N. Schatz, and W. G. Maisch, *J. Chem. Phys.* **60** (7), 2598 (1974).

Translated by G. Tsydynzhapov